Glycosylation structure and enzyme activity of lecithin:cholesterol acyltransferase from human plasma, HepG2 cells, and baculoviral and Chinese hamster ovary cell expression systems

Katherine R. Miller,[1] Jingchuan Wang, Mary Sorci-Thomas, Richard A. Anderson,* and John S. Parks[2]

Departments of Comparative Medicine and Internal Medicine,* The Bowman Gray School of Medicine of Wake Forest University, Medical Center Boulevard, Winston-Salem, NC 27157

Abstract The glycosylation state of lecithin:cholesterol acyltransferase (LCAT) may be important in determining its enzymatic activity. We compared glycosylation structure, enzyme kinetics, and phosphatidylcholine (PC) acyl specificity of human LCAT from four sources: human plasma (pLCAT), media from HepG2 cells (HepG2 LCAT), media from SF21 cells infected with a recombinant baculovirus (bLCAT) and media from stably transfected Chinese hamster ovary (CHO) cells (CHO LCAT). bLCAT was underglycosylated (molecular weight ~50 kDa) and resistant to digestion by N-glycanase F, endoglycosidase F, and neuraminidase. CHO and HepG2 LCAT were overglycosylated (~68 kDa and ~70–75 kDa) compared to pLCAT (~65 kDa). CHO LCAT, like pLCAT, was sensitive to N-glycanase F and neuraminidase but not to endoglycosidase F. HepG2 LCAT demonstrated resistance to N-glycanase F and endoglycosidase F. Apparent K_m values for all four enzymes were similar (1.4–9.2 μM cholesterol) for recombinant high density lipoproteins (rHDL) containing *sn*-1 16:0, *sn*-2 18:1 PC (POPC). Apparent V_{max} values (nmol cholesteryl ester formed/h per μg) were 52.6 for pLCAT, 48.6 for CHO LCAT, 15.3 for bLCAT, and 8.3 for HepG2 LCAT. Changes in PC acyl specificity in the presence and absence of cholesterol were characterized by comparing the ratio of LCAT activity on rHDL containing *sn*-1 16:0, *sn*-2 20:4 PC (PAPC) or POPC (PAPC/POPC activity ratio). The ratios for pLCAT, bLCAT, CHO LCAT, and HepG2 LCAT activity were 0.63, 0.49, 0.56, and 0.51 with cholesterol and 0.34, 0.29, 0.36, and 0.99 without cholesterol, respectively. We conclude that LCAT source influences glycosylation structure, which affects the apparent V_{max} for cholesteryl ester formation with only minor changes in apparent K_m or acyl substrate specificity.—**Miller, K. R., J. Wang, M. Sorci-Thomas, R. A. Anderson, and J. S. Parks.** Glycosylation structure and enzyme activity of lecithin:cholesterol acyltransferase from human plasma, HepG2 cells, and baculoviral and Chinese hamster ovary cell expression systems. *J. Lipid Res.* 1996. **37:** 551–561.

Supplementary key words LCAT • phosphatidylcholine

N-linked glycosylation is one of the structural components of lecithin:cholesterol acyltransferase (LCAT) that can potentially influence substrate binding and catalytic function. LCAT is secreted by hepatocytes into plasma as a 63–67 kilodalton glycoprotein, ~40% of which is carbohydrate (1–3). This enzyme has four N-linked glycosylation sites, N20, N84, N272, and N384. Previous experiments have shown that all four sites are utilized (2, 4). Digestion of plasma-derived LCAT by N-glycanase F produced a single band at 46 kilodaltons, the size of the protein backbone with no carbohydrate, suggesting that no O-linked carbohydrate was present (5). However, a more recent study using mass spectrometry analysis suggests that there are two O-linked carbohydrate residues on LCAT (6). Collet and Fielding (5) also demonstrated LCAT sensitivity to endoglycosidase F digestion that produced two bands, suggesting that LCAT was heterogeneously glycosylated. Neuraminidase digests of LCAT suggested a high sialic acid content as well (2, 5).

Several studies have examined the relationship between glycosylation of LCAT and enzymatic activity. Using CHO cells, Collet and Fielding (5) demonstrated that inhibitors of endoplasmic reticulum glucosidases

Abbreviations: LCAT, lecithin:cholesterol acyltransferase; pLCAT, plasma-derived LCAT; bLCAT, baculoviral-expressed LCAT; CHO LCAT, Chinese hamster ovary cell-expressed LCAT; HepG2 LCAT, HepG2 cell-expressed LCAT; HDL, high density lipoprotein; POPC, *sn*-1 palmitoyl, *sn*-2 oleoyl phosphatidylcholine; PAPC, *sn*-1 palmitoyl, *sn*-2 arachidonyl phosphatidylcholine; DPPC, dipalmitoyl phosphatidylcholine; rHDL, recombinant HDL.

[1]Present address: Susquehanna University, Department of Chemistry, Selinsgrove, PA 17870.

[2]To whom correspondence should be addressed.

Downloaded from www.jlr.org by guest, on June 18, 2012

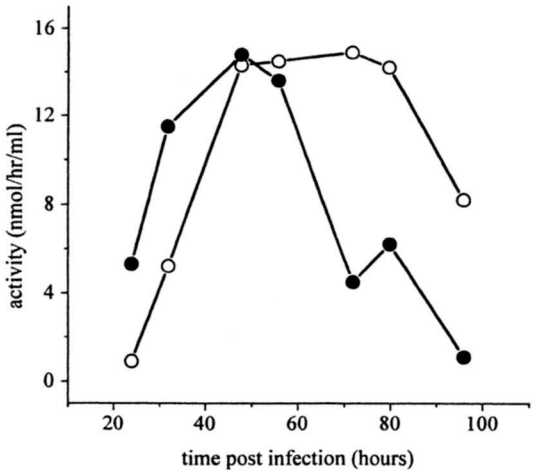

Fig. 1. Baculoviral LCAT expression time course at multiplicity of infection = 0.1 (open circles) and 5.0 (closed circles). Cultures consisting of 2.5×10^6 cells/ml in serum-free medium (SF900-II, Gibco) were infected with AcMNPV-LCAT at 0.1 or 5 plaque forming units/cell. One ml aliquots of medium were taken at 24, 32, 48, 56, 72, 80, and 96 h post infection and assayed for LCAT activity at 1.0 μM recombinant HDL substrate cholesterol concentration as described in Methods.

significantly reduced LCAT activity without reducing secreted enzyme mass. In contrast, inhibitors to microsomal and Golgi mannosidases had little effect on LCAT activity or secreted mass. Mutation of each glycosylation site has demonstrated the importance of glycosylation with respect to LCAT activity. Mutation of N84 and N272 in several experiments (4, 7, 8) caused significant reduction in activity, whereas mutation of N384 either caused an increase in LCAT specific activity (4, 8) or no change (7). Mutation of N20 caused only a slight decrease in specific activity (4, 7, 8).

Studies of LCAT function have used LCAT obtained from various sources: plasma-derived, CHO cell-expressed, Cos cell-expressed, and HepG2 cell-expressed LCAT. However, several studies have demonstrated that protein glycosylation can vary with cell type, species, and the state of differentiation (9, 10). Also, each glycosylation site in a protein can be processed differently depending on the local structure around the site (11, 12). The experiments described here characterize differentially glycosylated LCAT enzymes derived from human plasma, stably transfected CHO cells, SF21 cells infected with LCAT-encoded baculovirus, and HepG2 cells. Enzyme fatty acyl specificity and enzyme kinetics for recombinant HDL substrates were examined to determine the influence of differential glycosylation on enzyme function.

METHODS

Expression of LCAT in baculoviral system

Plasmid construction. LCAT cDNA was removed from pUC.LCAT (gift from J. McLean, Genentech Inc.) by digestion with Eco RI and Bam HI. The 1.4 kb fragment was electroeluted from a 1% agarose gel, and T4 DNA polymerase was used to fill in the ends. The LCAT fragment was blunt end-ligated to similarly treated pBlueBac II plasmid (pBBII, Invitrogen) and used to transform *E. coli* DH5α. Colonies were screened using a ^{32}P-labeled LCAT cDNA fragment. Positive colonies were selected, and the LCAT cDNA sequence and orientation in the vector were confirmed by Kpn I digestion and agarose electrophoresis and by dideoxy sequencing (13).

Transfection and plaque purification. Transfection of pBBII-LCAT and linear wild type AcMNPV baculoviral DNA was done according to Invitrogen protocols. Briefly, 2×10^6 SF9 cells (a cell line derived from *Spodoptera frugiperda* ovary cells) on a 60-mm plate were transfected with 3 μg pBBII-LCAT, 1 μg linear wild type AcMNPV, and 20 μl cationic liposomes in 1 ml Grace's medium (Invitrogen). After 4 h at 27°C, 1 ml complete TNM-FH medium (Invitrogen) was added, and the plates were incubated another 48 h at 27°C. The harvested medium contained both wild type and recombinant virus. The virus titer was increased by plating 1×10^6 SF9 cells/well in a 6-well plate, and adding 0.5 ml of a 1:10 dilution of transfection medium into SF900-II medium (Gibco). After 4 days at 27°C, the medium was harvested, and the cells were tested for β-galactosidase activity according to Gibco protocols. The cells were fixed in 2 ml formalin fixative (2% formaldehyde, 0.2% glutaraldehyde in phosphate-buffered saline) for 5 min at room temperature. After washing the cells two times with saline, 1 ml of an X-gal solution consisting of 100 mM potassium ferricyanide, 100 mM potassium ferrocyanide, 1 M magnesium chloride, and 20 mg/ml X-gal

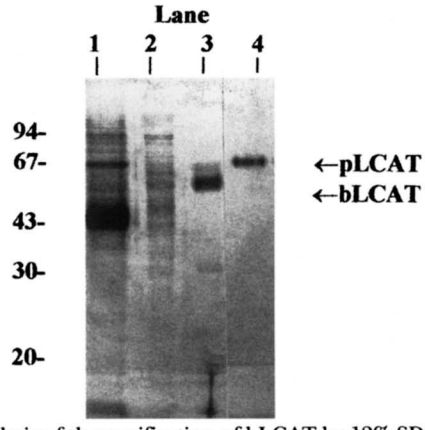

Fig. 2. Analysis of the purification of bLCAT by 12% SDS-PAGE. In order to detect all possible contaminants, the electrophoresis was stopped before the dye front reached the bottom of the gel. The gel was subsequently silver stained. The LCAT was expressed in SF21 cells at 0.1 MOI for 72 h. The medium was supplemented with 0.02% ovalbumin in order to reduce enzyme degradation. Lane 1, whole medium; lane 2, LCAT-active phenyl-Sepharose pool; lane 3, LCAT-active hydroxylapatite flow through; lane 4, purified plasma LCAT.

Downloaded from www.jlr.org by guest, on June 18, 2012

TABLE 1. Purification scheme for baculoviral-expressed lecithin:cholesterol acyltransferase

Sample	Total Activity	Total Mass	% Yield by Activity	Specific Activity
	nmol CE/h	μg		*nmol CE/h/μg*
Medium	20,440 ± 1644	nd	100	nd
Phenyl-Sepharose pool	5092 ± 1792	83 ± 55	24.6 ± 9.2	80.3 ± 42.6
Hydroxylapatite flow through	212 ± 198	113 ± 69	1.0 ± 0.9	1.9 ± 1.3
Concentrated LCAT	1197 ± 967	58 ± 54	20.0 ± 28.9	48.8 ± 27.3

Values are means ± SD of four purification runs. Activity was measured at saturating substrate concentrations (1.2 μg cholesterol/reaction) as described in Methods. Protein mass was measured using slot-blot analysis as described in Methods; nd, mass was not measured due to medium components interfering with the assay; CE, cholesteryl ester.

(Sigma) in phosphate-buffered saline was added to the plate. After incubation for 4 h at room temperature, cells infected by recombinant virus turned blue.

Two rounds of plaque purification were performed by plating 2×10^6 SF9 cells per well in a 6-well plate and adding 2 ml virus stock diluted from 10^{-2} to 10^{-8} in SF900-II medium to the cells. After 1 h at room temperature, the medium was removed, and 2 ml 1% agarose containing Bluegal (Gibco) in SF900-II medium was plated onto the cells. The plates were incubated for 4–7 days at 27°C until plaques appeared. Blue recombinant plaques were picked with a sterile pipet tip and placed in 0.5 ml SF900-II medium to elute the virus. This virus was used to repeat the plaque purification. A working stock of the purified recombinant virus was made by infecting a 15-ml suspension culture of SF9 cells in SF900-II medium with a plaque and incubating at 27°C for 5 days. The harvested medium was titered by a plaque assay, which also confirmed the purity of the virus stock. Titers of $1–2 \times 10^8$ plaque-forming units were achieved. The virus stocks were stored at 4°C in foil-covered tubes.

Baculoviral LCAT expression and purification

SF21 cells were grown to a density of 2.5×10^6 cells/ml in SF900-II medium. The cells were pelleted and resuspended in fresh medium at a density of 5×10^6 cells/ml. Cultures of 100 ml in 500-ml Erlenmeyer flasks were routinely infected at a multiplicity of infection (MOI) of 0.1, and 0.02% albumin (from a 35% sterile, tissue culture grade solution from Sigma) or 0.02% ovalbumin (Sigma) was added to the culture to stabilize the expressed LCAT. The culture was incubated at 27°C on an orbital shaker set at 150 rpm. The medium was harvested at 72 h post infection by centrifuging at 1500 *g* for 15 min. The medium was adjusted to 0.5 M NaCl, cooled to 4°C, and loaded onto a 1 × 9 cm phenyl-Sepharose column equilibrated in 4 mM sodium phosphate, pH 7.4, 0.5 M NaCl at a flow rate of 1.5 ml/min. The column was washed with 3–4 column volumes of the equilibration buffer and eluted with 8 volumes of deionized water. Protein-containing fractions were pooled and adjusted to 4 mM sodium phosphate, pH 6.9, and loaded onto a 1 × 9 cm hydroxylapatite column equilibrated with 4 mM sodium phosphate, pH 6.9, at a flow rate of 1 ml/min. The LCAT-containing flow-through and wash was collected, adjusted to 10% glycerol, and concentrated in an Amicon pressure concentrator with a YM30 membrane. The concentrated LCAT was aliquoted and stored at -70°C under argon. The activity of LCAT stored in this manner was stable for at least 6 months.

Treatment of infected SF21 cells with tunicamycin

Cells were infected with LCAT virus as described above. At 24 h post infection, tunicamycin was added to the culture to a concentration of 2 μg/ml. Medium was harvested at 72 h post infection. Whole medium was run on 12% SDS-polyacrylamide gels and visualized by Western blotting.

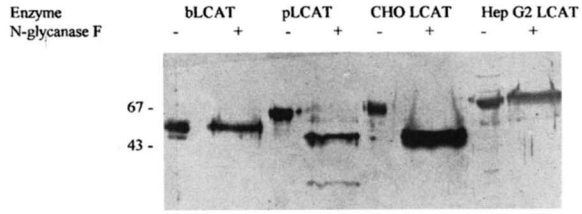

Fig. 3. Western blot analysis of N-glycanase F (NGF) digestion of plasma-derived LCAT (pLCAT), baculoviral- (bLCAT), CHO- and HepG2-expressed LCAT. Purified bLCAT, purified pLCAT, CHO medium, and HepG2 medium were incubated overnight as described in Methods. Proteins were separated by 12% SDS-PAGE and Western blotted. Goat anti-LCAT polyclonal antibody was used to probe the blot. From left to right: lane 1, bLCAT; lane 2, bLCAT + NGF; lane 3, pLCAT; lane 4, pLCAT + NGF; lane 5, LCAT transfected CHO medium; lane 6, LCAT transfected CHO medium + NGF; lane 7, HepG2 medium; lane 8, HepG2 medium + NGF. The presence of detergent on the NGF incubations results in a wider banding pattern on the gels.

Downloaded from www.jlr.org by guest, on June 18, 2012

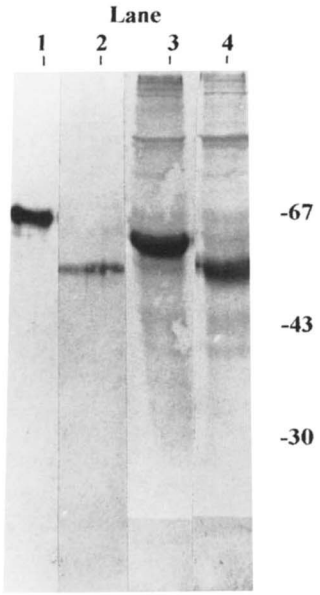

Fig. 4. Western blot analysis of bLCAT expressed in the presence of tunicamycin. Purified plasma LCAT and baculoviral medium grown in the absence or presence of 2 μg/ml tunicamycin were separated by 12% SDS-PAGE and Western blotted. The Western blot was probed with an goat anti-LCAT polyclonal antibody. Lane 1, purified pLCAT; lane 2, pLCAT + N-glycanase F; lane 3, bLCAT medium without tunicamycin; lane 4, bLCAT medium in the presence of tunicamycin.

Expression of LCAT by Chinese hamster ovary (CHO) cells

CHO cells obtained from ATCC were grown in equal volumes of Dulbecco's modified Eagle's medium and Coon's F12 medium, supplemented with 10% fetal bovine serum and essential amino acids, at 37°C in a 5% CO_2 atmosphere. Transfections were performed using a modification of the calcium chloride precipitation method (14). Human wild-type LCAT cDNA (kindly provided by J. McLean, Genentech) was transferred into pCMV-5 using the Bam HI and Eco RI restriction sites. pCMV-LCAT was mixed with herring sperm DNA (ratio of 2:1) and cotransfected with pSV2neo at a ratio of 10:1. Briefly, the DNA mixture was precipitated with calcium chloride as described (14) and allowed to incubate with the cells overnight. Once cells had become confluent, stably expressing CHO cells were selected by adding G418 (Gibco) at a concentration of 550 μg/ml to the medium. The antibiotic-resistant cells were then selected over a 2-week period. Six independent clones were tested for LCAT activity using an rHDL substrate containing phosphatidylcholine–cholesterol–apoA-I (100:5:1). One of the lines, CHO LCAT #5, showed the highest level of initial enzyme velocity at 19.5 nmol cholesteryl ester formed/h per ml. To obtain human LCAT activity for use in LCAT assays, stable expressing CHO cells were grown to approximately 75% confluence in 100-mm dishes, the cell monolayer was washed with phosphate-buffered saline, and serum-free medium was then applied. The conditioned medium was removed approximately 72 h later and spun to remove cell debris. Aliquots of the medium were then frozen at -20°C until used in the LCAT assay.

Purification of plasma LCAT

LCAT was purified from fresh recovered human plasma obtained from the Red Cross by following a modification of the procedure published by Chen and Albers (15). Plasma lipoproteins were precipitated with dextran sulfate–Mn^{+2} as described. LCAT was purified from the lipoprotein-free plasma by adjusting the plasma to 4 M NaCl and loading the plasma onto a 2.5 × 23 cm phenyl-Sepharose column equilibrated with 50 mM Tris (pH 7.4), 150 mM NaCl. The column was washed with the same buffer until the OD_{280} dropped below 0.3. LCAT was eluted from the column with water. The protein pool was adjusted to 10 mM Tris (pH 7.4), 25 mM NaCl and was loaded onto a 2.5 × 23 cm DEAE-Sepharose column. The column was eluted using a 900 ml linear gradient of 10 mM Tris (pH 7.4), 25–250 mM NaCl. LCAT active fractions were pooled, concentrated, and adjusted to 4 mM sodium phosphate buffer, pH 7.0, 150 mM NaCl, and loaded onto a 1.5 × 20 cm hydroxylapatite column. A 400 ml linear gradient from 4 mM sodium phosphate to 60 mM sodium phosphate, 150 mM NaCl was used to elute the enzyme from the column. The LCAT active fraction was pooled, concentrated, adjusted to 20% glycerol, and stored at -70°C. This procedure resulted in pure LCAT as determined by SDS-PAGE and silver staining (see Results).

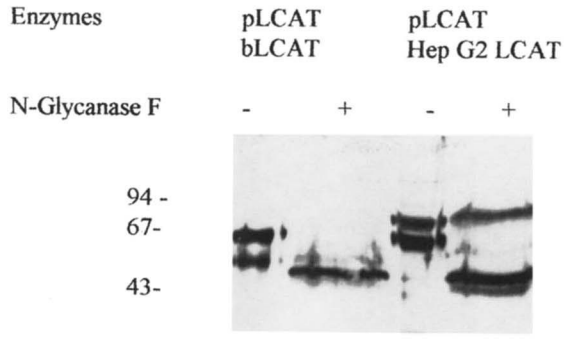

Fig. 5. Western blot analysis of pLCAT digestion by N-glycanase F (NGF) in presence of purified bLCAT and HepG2 medium. bLCAT and HepG2 medium were mixed with pLCAT and digested by NGF overnight as described in Methods. The proteins were separated by 12% SDS-PAGE and Western blotted. The Western blot was probed by a goat anti-LCAT polyclonal antibody. From left to right: lane 1, pLCAT and bLCAT mixed; lane 2, pLCAT and bLCAT mixed and digested with NGF; lane 3, HepG2 medium and pLCAT mixed; lane 4, HepG2 medium and pLCAT mixed and digested with NGF. Presence of detergent in the N-glycanase F incubations results in a wider banding pattern on the gels (lanes 2 and 4).

Downloaded from www.jlr.org by guest, on June 18, 2012

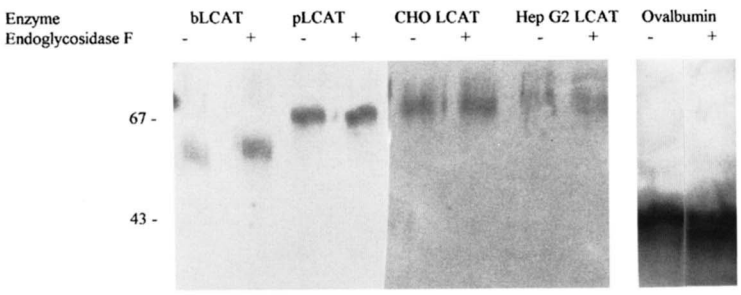

Fig. 6. Western blot analysis of LCAT digestion by endoglycosidase F (endo F). pLCAT, bLCAT, CHO LCAT medium, and HepG2 medium were digested with endo F at 37°C overnight. The proteins were run on a 7.5% SDS gel, and lanes 1–8 were Western blotted. A chicken anti-LCAT antibody was used to visualize the enzyme in the Western blots. Lanes 9 and 10 were silver stained. From left to right: lane 1, bLCAT; lane 2, bLCAT + endo F; lane 3, pLCAT; lane 4, pLCAT + endo F; lane 5, CHO LCAT; lane 6, CHO LCAT + endo F; lane 7, HepG2 LCAT; lane 8, HepG2 LCAT + endo F; lane 9, ovalbumin; lane 10, ovalbumin + endo F.

Recombinant HDL synthesis

Recombinant HDL (rHDL) consisting of phosphatidylcholine (PC), apolipoprotein A-I (apoA-I) with or without [^{14}C]cholesterol were formed by the sodium cholate dialysis method initially described by Matz and Jonas (16). The cholesterol-containing rHDL were used to measure cholesterol esterification by LCAT whereas the cholesterol-free rHDL were used to measure the phospholipase A_2 activity of LCAT as release of radiolabeled free fatty acid from the *sn*-2 position of PC. The specific phosphatidylcholine used in the rHDL depended on the experiment. Egg yolk lecithin (Serdary) containing rHDL at a 55:2:1 molar ratio of PC:cholesterol:apoA-I was used to assay for activity during LCAT purifications. rHDL containing *sn*-1 palmitoyl, *sn*-2 oleoyl phosphatidylcholine (POPC, Sigma), [^{14}C]cholesterol (3.3×10^5 dpms/μg, NEN) and apoA-I (42:2.4:1 mole ratio) was used for the substrate saturation experiments. For the substrate specificity experiments, *sn*-1 palmitoyl, *sn*-2 [^{3}H]oleoyl phosphatidylcholine ([^{3}H]POPC) and *sn*-1 palmitoyl, *sn*-2 [^{3}H]arachidonyl phosphatidylcholine ([^{3}H]PAPC) were synthesized from [^{3}H]oleic acid (NEN) and [^{3}H]arachidonic acid (NEN), respectively, and lysophosphatidylcholine (Sigma) as previously described (17).

LCAT enzyme assay

LCAT activity was measured as cholesterol esterification as previously described (17). LCAT incubations were conducted in 500 μl buffer consisting of 140 mM sodium chloride, 10 mM Tris (pH 7.4), 0.01% sodium azide, 0.01% EDTA, 2% albumin, and 10 mM β-mercaptoethanol (final concentration) and the appropriate amount of rHDL and LCAT enzyme. The solution was mixed, overlaid with argon, and incubated for 1 h at 37°C. The reaction was stopped by the addition of 1.8 ml Bligh-Dyer extraction solution (18) consisting of chloroform–methanol 1:2 with 25 μg/ml of cholesterol and cholesterol oleate added. The phases were split upon addition of 0.7 ml chloroform and 0.7 ml 0.29% NaCl. The organic phase was dried, resuspended in 50 μl chloroform, and applied to a thin-layer chromatography plate, which was subsequently developed in a solvent of hexane–ether–acetic acid 70:30:2. Bands were visualized with iodine vapor and counted in a Beckman LS 7000 scintillation counter for 10 min. Cholesterol esterification was kept below 20% by adjusting the amount of LCAT enzyme to remain in the linear range of cholesteryl ester formation. LCAT specific activity was calculated by multiplying the fraction of cholesteryl ester formed by the nmol of cholesterol in each reaction and normalizing to 1 μg of LCAT.

The amount of cholesterol added in each incubation in the form of rHDL varied with the experiment. For LCAT activity measurements during purification, 1.2 μg cholesterol per incubation were used. For substrate saturation experiments, cholesterol was added at 0.2, 0.4, 0.6, 0.8, 1.0, and 1.5 μg per reaction; for substrate specificity reactions, 0.4 μg cholesterol per reaction was used.

LCAT phospholipase A_2 activity measurements

Phospholipase A_2 activity measurements used rHDL containing [^{3}H]POPC or [^{3}H]PAPC and no cholesterol. Each reaction contained 75 μg phospholipid. The samples were mixed, incubated, and processed in the same manner as the LCAT activity assays except for the extraction step. The incubation was stopped by the addition of 1.8 ml Bligh-Dyer extraction solution containing 25 μg/ml oleic acid and POPC. The phases were split upon addition of 0.7 ml chloroform and 0.7 ml 0.05% sulfuric acid. The samples were then processed as described above. After cutting the phospholipid band from the TLC plate, 400 μl water was added to elute the phospholipid. After 10 min at room temperature, the scintillation fluid was added, and the samples were counted. The phospholipase specific activity was calculated by multiplying the fraction of fatty acid formed by the nmoles of phospholipid in each reaction and normalizing to 1 μg LCAT.

Slot blot analysis of LCAT protein mass

A Schleicher and Schuell minifold II slot blot system was used to determine LCAT concentrations. A concen-

Downloaded from www.jlr.org by guest, on June 18, 2012

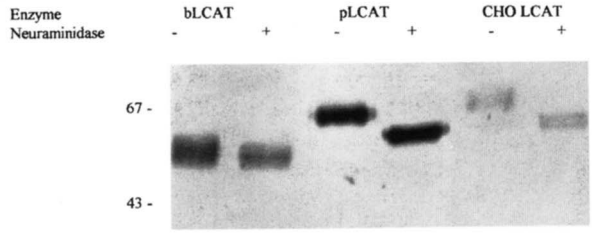

Fig. 7. Western blot analysis of neuraminidase-digested LCAT. Purified bLCAT, pLCAT, and CHO LCAT medium were digested as described. The proteins were separated by 7.5% SDS-PAGE and Western blotted. The Western blots were probed with a mouse anti-LCAT monoclonal antibody. From left to right: lane 1, purified bLCAT; lane 2, purified bLCAT + neuraminidase; lane 3, purified pLCAT; lane 4, purified pLCAT + neuraminidase; lane 5, CHO LCAT medium; lane 6, CHO LCAT medium + neuraminidase.

trated preparation of bLCAT standard and samples were prepared by diluting protein into 200 µl of 1% β-mercaptoethanol and boiling for 5 min. The wells of the assembled slot blot apparatus were rinsed with 10 mM phosphate, 150 mM NaCl, pH 7.4. The samples were loaded into the wells, and the solvent was pulled through the nitrocellulose under vacuum. The apparatus was disassembled, and the nitrocellulose was blocked for 1 h with 3% albumin (fraction V, Sigma) in a 10 mM Tris, 200 mM NaCl, pH 7.4, buffer at room temperature. Anti-LCAT monoclonal antibody 5D4 (gift from Dr. Yves Marcel, University of Ottawa Heart Institute, Ottawa, Ontario, Canada) was diluted 1:1000 in 1% albumin, 0.1% Triton X-100, 0.02% SDS in Tris-saline buffer. The blot was incubated for 1 h at room temperature and then washed in the same buffer without albumin. The secondary anti-mouse alkaline phosphatase conjugated antibody (Sigma) was added to the blot in the same buffer containing 1% albumin and incubated for 1 h at room temperature. The blot was washed in Tris-saline and developed in 10 ml of 100 mM Tris, 100 mM NaCl, 0.1% $MgCl_2 \bullet 6H_2O$, pH 9.6, supplemented with 60 µl of 50 mg/ml nitroblue tetrazolium (NBT, Promega) and 30 µl of 50 mg/ml 5-bromo-4-chloro-3-indolyl phosphate (BCIP, Promega). The blots were analyzed by laser densitometry, and a linear least squares line fit to the signal intensity from the standards was used to form the standard curve. The linear range of the slot blots was between 1 and 20 ng/well.

LCAT protein analysis

LCAT protein was separated on 12% SDS-polyacrylamide gels (19). Gels were silver stained by a modified Oakley method (20). Briefly, gels were fixed in 10% acetic acid, 25% isopropanol for 15 min. After washing in four changes of deionized water for 20 min, gels were soaked in 100 ml 30 mM dithiothreitol for 1 h at room temperature. Gels were then incubated for 15 min in a solution of 0.2 M ammonium hydroxide, 0.075% sodium hydroxide, 47 mM silver nitrate. The gels were washed in 3 changes of deionized water for a total of 10 min, then developed in 50 ml of 5 mM citric acid and 0.019% formaldehyde. Development was stopped by placing gels in 45% methanol, 3% acetic acid.

Western blots were produced by electroblotting proteins from gels onto nitrocellulose membranes. The blots were blocked overnight at 4°C in 5% nonfat dry milk in 10 mM Tris (pH 7.4), 200 mM NaCl. Anti-LCAT goat polyclonal antibody (gift from Dr. Henry Pownall, Baylor College of Medicine, Houston, Texas) was diluted 1:2000 or chicken anti-LCAT polyclonal antibody was diluted 1:7500 in 2.5% nonfat dry milk, 0.02% SDS, 0.1% Triton X-100 in Tris-saline buffer and incubated with the blot for 1.5 h at room temperature. After washing the blot in antibody buffer, rabbit anti-goat or rabbit anti-chicken antibodies conjugated to alkaline phosphatase (Sigma) were diluted 1:1000 or 1:5000, respectively, and incubated with the blot for 2 h at room temperature. The blot was then washed three times in Tris-saline for a total of 30 min. The LCAT was visualized with NBT and BCIP diluted in 100 mM Tris, 100 mM NaCl, 5 mM $MgCl_2 \bullet 6H_2O$, pH 9.6.

HepG2 cell culture

HepG2 cells were cultured in T75 flasks in the presence of 13 ml of minimal essential medium supplemented with L-glutamine, vitamins, penicillin, streptomycin, and 10% fetal bovine serum. These cells were maintained in a humidified 5% CO_2 atmosphere. LCAT was harvested by washing the cells two times with a balanced salt solution and then incubating 48 h in the presence of the medium without serum added.

Deglycosylation of LCAT

N-glycanase F (Boehringer Mannheim) treatment of LCAT was performed as follows: 1 µl of 10% SDS was added to 500 ng purified pLCAT or 500 ng purified bLCAT in 20 µl water, or 20 µl CHO medium, or 20 µl HepG2 medium and denatured by boiling for 5 min. The solution was then adjusted to 40 mM potassium phosphate, pH 7.4, 40 mM EDTA. Nonidet-P40 was added to 0.9%, and the mixture was brought to 40 µl with water. N-glycanase F (0.6 units) was added, and the protein was incubated 15 h at 37°C. The deglycosylated protein was run on a 12% SDS-polyacrylamide gel, and the LCAT was visualized by Western blotting.

Endoglycosidase F (Boehringer Mannheim) treatment of LCAT was performed as follows: 500 ng pLCAT, 500 ng bLCAT, 20 µl CHO medium, 20 µl HepG2 medium, or 500 ng ovalbumin were adjusted to 1.5% β-mercaptoethanol and denatured by boiling for 5 min. The following was then added: 1.6 µl 3 M sodium acetate, pH 6.0, 2.7 µl 5% EDTA, and 2 µl (0.1 units)

Downloaded from www.jlr.org by guest, on June 18, 2012

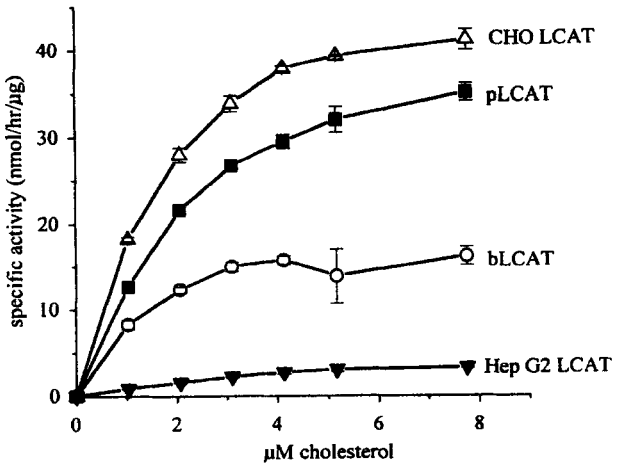

Fig. 8. Substrate saturation of pLCAT, bLCAT, CHO LCAT, and HepG2 LCAT. Recombinant HDL disks containing POPC, cholesterol, and apoA-I in a molar ratio of 42:2.4:1 were assayed at 0.2, 0.4, 0.6, 0.8, 1.0, and 1.5 µg cholesterol/reaction for 1 h at 37°C. The cholesterol esterification per µg LCAT is reported. Points are the mean ± standard deviation of three replicates using purified pLCAT, purified bLCAT, CHO LCAT medium, and HepG2 medium as sources of enzyme.

N-glycanase free, endoglycosidase F. The reactions were incubated at 37°C overnight, run on a 7.5% SDS-polyacrylamide gel, and the LCAT was visualized by Western blotting. The ovalbumin was visualized by silver staining.

Neuraminidase (New England Biolabs) treatment of LCAT was performed as follows: 20 µl CHO medium was used or 500 ng pLCAT or 500 ng bLCAT were diluted to 20 µl with water. Two µl of 10× reaction buffer (500 mM sodium citrate, pH 4.5) and 1 µl (50 units) neuraminidase were added before the protein was digested overnight at 37°C, run on an SDS gel, and visualized by Western blotting.

RESULTS

Baculoviral expression systems have been used to produce mass quantities of proteins and enzymes that require posttranslational modification. An LCAT baculoviral expression vector was constructed to produce mass amounts of LCAT for physical studies. LCAT cDNA was cloned into the BlueBac II transfection vector (Invitrogen), which replaced the polyhedron gene with LCAT upon recombination with linearized AcMNPV virus. High titer, LCAT-expressing virus was isolated after three rounds of plaque purification and screening. Using this stock, LCAT expression was examined as a function of the incubation time and the multiplicity of infection (MOI). **Figure 1** shows LCAT expression time courses at MOIs of 0.1 and 5.0. Both MOIs produced the same amount of activity in the medium. However, cell lysis rapidly occurred after 48 h in the 5.0 MOI culture, resulting in LCAT degradation, whereas lysis did not become significant until after 80 h in the 0.1 MOI culture. As the time window for harvesting maximum LCAT activity is greater, an MOI of 0.1 and an incubation time of 72 h were chosen for the expression of LCAT in serum-free-medium.

Purification of the baculoviral-expressed LCAT (bLCAT) required only two column steps to produce pure LCAT protein. The medium was harvested from the cells by centrifugation at 1500 *g* for 15 min. One hundred fifty ml of medium was adjusted to 0.5 M NaCl, and loaded onto a 5-ml phenyl-Sepharose column. After washing, LCAT activity was eluted by passing deionized water over the column. The use of 1–5% ethanol increased enzyme yield but irreversibly inactivated the protein (data not shown). The protein was pooled, adjusted to 4 mM sodium phosphate, pH 6.9, and passed through a 5-ml hydroxylapatite column. At this low phosphate concentration most of the bLCAT flowed through the column, whereas the remaining contaminants were almost completely bound. The hydroxylapatite flow through was adjusted to 10% glycerol, concentrated, and immediately frozen at -70°C.

Purification of bLCAT was monitored by SDS-PAGE, immunoreactive LCAT mass, and LCAT activity (**Fig. 2** and **Table 1**). As shown in Fig. 2, the harvested medium contained contaminating proteins, many of which were removed by a phenyl-Sepharose column (lane 1, lane 2). This column also functioned to exchange the buffer and concentrate the enzyme. The hydroxylapatite column further purified LCAT (lane 3) to > 90% purity. Table 1 summarizes the purification of LCAT at each step for four purifications. This method of purifying LCAT resulted in an overall 20% yield. The only significant loss of LCAT protein mass occurred at the phenyl-Sepharose step due to incomplete elution from the column. However, LCAT specific activity continued to decrease until the hydroxylapatite flow through was concentrated, where much of the lost activity was regained. The resultant purified bLCAT had a specific activity of 48.8 nmol cholesteryl ester formed/h per µg enzyme when activity was measured at saturating substrate cholesterol concentrations. The specific activity of the medium could not be measured as overwhelming amounts of other proteins interfered with the slot blot assay, resulting in an underestimate of bLCAT mass. A comparison of bLCAT (lane 3) and pLCAT (lane 4) in Fig. 2 shows that the molecular weight of bLCAT is approximately 50 kilodaltons, which is distinctly smaller than pLCAT. This difference in molecular weight between baculoviral-ex-

Downloaded from www.jlr.org by guest, on June 18, 2012

TABLE 2. Apparent V_{max} and apparent K_m for LCAT from plasma, baculoviral, CHO, and HepG2 sources

Enzyme	Apparent K_m	Apparent V_{max}
	μM	*nmol CE formed/h/μg*
pLCAT	3.8	52.6
bLCAT	1.4	19.6
CHO LCAT	2.1	55.6
HepG2 LCAT	9.0	8.3

Disk composition (molar ratio), POPC–cholesterol–apoA-I 42.0:2.4:1. CE, cholesteryl ester.

pressed LCAT and plasma-derived LCAT was also observed by Chawla and Owen (21) in their baculoviral-expressed LCAT.

To investigate differences in glycosylation among several sources of LCAT, plasma-derived LCAT and cell culture-expressed LCAT were digested with several glycosidases. N-glycanase F (NGF) removes all N-linked carbohydrate by cleaving between the asparagine and the first N-acetylglucosamine moiety on the carbohydrate chain. **Figure 3** shows the molecular weights of bLCAT, pLCAT, LCAT secreted from transfected CHO cells (CHO LCAT) and LCAT secreted from HepG2 cells (HepG2 LCAT). Each LCAT had a distinct mobility on SDS-PAGE before and after NGF digestion. bLCAT, with a molecular weight of ~50 kilodaltons, was resistant to NGF digestion (lanes 1 and 2), as was HepG2 LCAT (molecular weight ~75 kilodaltons, lanes 7 and 8). pLCAT (molecular weight ~65 kDa, lanes 3 and 4) and CHO LCAT (molecular weight ~68 kDa, lanes 5 and 6) were both sensitive to NGF. To show that bLCAT contained N-linked carbohydrate, bLCAT was expressed in the presence of 2 μg/ml tunicamycin, which inhibits all N-linked glycosylation. The LCAT produced had a molecular weight of ~46 kDa, the size expected for the unglycosylated protein transcript (**Fig. 4,** lanes 2 and 3). To rule out the possibility that an inhibitor of N-glycanase F was copurified with the baculoviral-expressed LCAT or was present in the HepG2 medium, we performed a mixing experiment in which purified plasma LCAT was added to the purified bLCAT or to the medium from HepG2 cells and digested with N-glycanase F (**Fig. 5**). As shown in lanes 2 and 4, the pLCAT was reduced in size, whereas the bLCAT (lane 2) and HepG2 LCAT (lane 4) remained unchanged, indicating that the carbohydrate structures of bLCAT and HepG2 LCAT are distinct from those of pLCAT and CHO LCAT.

Further evaluation of the carbohydrate structure of these enzymes was performed with endoglycosidase F (endo F) and neuraminidase. Endo F cleaves between the first and second sugar group in high-mannose carbohydrate chains. Digestion with an endo F preparation free of N-glycanase F, as shown in **Fig. 6,** resulted in no change in molecular weight for any of the examined enzymes whereas ovalbumin, a protein sensitive to endo F, was reduced in size under the same incubation conditions (lanes 9 and 10). This result indicates that all carbohydrate chains were processed beyond the high-mannose stage for each enzyme. Neuraminidase is an exoglycosidase that removes terminal sialic acid residues from carbohydrate chains. Digestion of LCAT with neuraminidase, as shown in **Fig. 7,** resulted in a decreased molecular weight for pLCAT (lanes 3 and 4) and CHO LCAT (lanes 5 and 6). However, bLCAT (lanes 1 and 2) was resistant to neuraminidase treatment.

In view of these observed differences in glycosylation patterns, enzyme kinetics were compared to determine whether glycosylation patterns affected LCAT activity. Substrate saturation experiments, as shown in **Fig. 8,** were done with each enzyme using rHDL consisting of POPC, cholesterol, and apoA-I (42:2.4:1 molar ratio). The apparent K_m and apparent V_{max} values are shown in **Table 2.** The apparent K_m of CHO LCAT was between that of pLCAT and bLCAT. bLCAT had a smaller apparent K_m than that of pLCAT, whereas HepG2 LCAT displayed a larger apparent K_m. The apparent V_{max} values of pLCAT and CHO LCAT were similar (53–56 nmol/h per μg), whereas the apparent V_{max} values of bLCAT and HepG2 LCAT were greatly reduced.

The fatty acyl substrate specificity of each LCAT was examined in the presence and absence of cholesterol by comparing the activities of the enzymes on recombinant HDL disks consisting of POPC:cholesterol:apoA-I (43:3.7:1 molar ratio), PAPC:cholesterol:apoA-I (50:2.9:1 molar ratio), [^{3}H]POPC:apoA-I (65:1 molar ratio) and [^{3}H]PAPC:apoA-I (52:1 molar ratio). The ratio of PAPC to POPC specific activities was calculated for each enzyme (**Table 3**). In comparison to pLCAT, bLCAT demonstrated a decreased reactivity with POPC and PAPC under all conditions. In the absence and presence of cholesterol, the PAPC/POPC activity ratio was decreased for bLCAT. In contrast, CHO LCAT demonstrated a similar reactivity with both POPC and PAPC, resulting in similar PAPC/POPC activity ratios. HepG2 LCAT demonstrated low activity against both POPC and PAPC in the presence of cholesterol and high phospholipase activity in the absence of cholesterol. The phospholipase activity may be due to other phospholipases secreted by the HepG2 cells (22). Conditioned media from untransfected CHO cells were used as a control for the CHO LCAT experiments and were similar to the no enzyme controls (data not shown). Except for the HepG2 LCAT, the ratio of phospholipase to transacylase activity was not altered in either of the expressed enzymes compared to pLCAT.

Downloaded from www.jlr.org by guest, on June 18, 2012

TABLE 3. LCAT activities with PAPC and POPC recombinant HDL

LCAT Source	Cholesterol Esterification[a] POPC[b]		PAPC	Activity Ratio PAPC/POPC
	nmol CE formed/h/ml			
pLCAT	9.3 ± 1.1	(n=5)	5.9 ± 0.4	0.63
bLCAT	4.5 ± 0.6	(n=5)	2.2 ± 0.05	0.49
CHO LCAT	10.3 ± 0.9	(n=5)	5.8 ± 0.7	0.56
HepG2 LCAT	0.63 ± 0.02		0.32 ± 0.05	0.51
	Phospholipase A_2 Activity[d] POPC[e]		PAPC[f]	
	nmol FA released/h/ml			
pLCAT	35.7 ± 2.2		12.0 ± 3.9	0.34
bLCAT	16.1 ± 3.2		4.7 ± 1.9	0.29
CHO LCAT	32.4 ± 2.4		11.6 ± 4.1	0.36
HepG2 LCAT	14.3 ± 1.5		14.1 ± 4.8	0.99

[a]All values are the mean ± SD of three replicates unless otherwise indicated.
[b]Disk composition was 43:3.7:1 molar ratio of POPC–cholesterol–apoA-I; 0.4 μg cholesterol and 9.1 μg POPC were used in each reaction.
[c]Disk composition was 50:2.9:1 molar ratio of PAPC–cholesterol–apoA-I; 0.4 μg cholesterol and 13.9 μg PAPC were used in each reaction.
[d]All values are the mean ± SD of three replicates.
[e]Disk composition was 65:1 molar ratio of POPC–apoA-I; 75 μg of POPC was used in each reaction.

DISCUSSION

The purpose of this study was to characterize the glycosylation structure and enzyme function of LCAT from baculoviral and CHO cell expression systems, human plasma, and media of HepG2 cells. The glycosylation of LCAT by the baculoviral expression system and HepG2 cells was structurally different from the glycosylation of human plasma LCAT. The difference in glycosylation affected enzyme kinetics by reducing the apparent V_{max} of the enzyme, with only minor changes in the apparent K_m. Differences in glycosylation may have minor influences on LCAT fatty acyl substrate specificity. Overall, CHO cell-expressed LCAT was most similar to plasma-derived LCAT.

Detailed study of the enzymatic mechanism of LCAT requires a source of mass quantities of enzyme. Expression of LCAT in the baculoviral system produced active enzyme, which was purified in two column steps. Based on purified bLCAT specific activity, medium concentrations of 1.5–3.0 μg/ml were readily achieved. By silver-stained SDS gels, the described purification of this enzyme using phenyl-Sepharose and hydroxylapatite columns produced 90–100% pure LCAT. This purification protocol is simpler and less time-consuming than the purification of pLCAT and is without risk of apolipoprotein contamination. However, although the baculoviral system expressed significant quantities of LCAT, the expressed enzyme is underglycosylated compared to the plasma-purified enzyme. Expression in the presence of tunicamycin demonstrated that the change in molecular weight was due to underglycosylation, not truncation of the protein transcript. There have been similar reports of underglycosylated proteins expressed in insect cell lines (23). The extent and type of glycosylation often is different in baculoviral-expressed proteins. Patterns of glycosylation in insect cells have been shown to vary with cell line, culture medium, culture supplements, time after infection, and the protein expressed (23).

The underglycosylation of bLCAT led to a further examination of LCAT expressed by several commonly used cell lines. CHO LCAT, like pLCAT, was sensitive to N-glycanase F and was only slightly overglycosylated compared to pLCAT. HepG2 LCAT was overglycosylated and, like bLCAT, was resistant to N-glycanase F, suggesting that the carbohydrate composition was different from that of pLCAT. Resistance to N-glycanase F has been observed only in a few plant proteins that contained an α(1 → 3)fucose on the N-acetylglucosamine moiety proximal to the asparagine (24). However, α(1 → 6)fucosylation at this same moiety is easily hydrolyzed (24). Fucosyl transferase activity has been observed in insect cells and may explain the resistance of bLCAT to N-glycanase F (23). Unlike the results of Collet and Fielding (5), we found all forms of LCAT resistant to endo F. For these experiments, N-glycanase F-free endo F was used. Partial digestion by a small amount of N-glycanase F, a common contaminant of endo F, may explain the previously published results (5).

Downloaded from www.jlr.org by guest, on June 18, 2012

The results of the endo F experiment indicate that all carbohydrate structures were processed beyond the high mannose stage, supporting a recently published study using mass spectroscopy to characterize the glycosylation structure of LCAT (6). This study demonstrated that the N-linked glycosylation in plasma LCAT was processed beyond the high mannose stage and contained sialylated triantennary and biantennary complex structures. Two O-linked glycosylation sites in LCAT (T407 and S409) were also identified. However, our methods were not sensitive enough to detect the small differences in molecular size that would have resulted if LCAT were underglycosylated at the O-linked sites.

Both pLCAT and CHO LCAT were sensitive to neuraminidase, indicating that both enzymes contained terminal sialic acid residues. In contrast, bLCAT demonstrated no significant change in molecular weight upon neuraminidase digestion. This result suggests that the baculoviral LCAT contained little or no terminal sialic acid residues. Although glucosidase and mannosidase activities can be detected in insect cells, processing beyond hybrid structures usually is not observed (23). Galactosyl and sialyl transferase activities are negligible, and proteins generally lack terminal sialic acid residues (23). Therefore, sensitivity to neuraminidase would not be expected for bLCAT. On the basis of the carbohydrate analysis of these four enzymes, CHO LCAT is most similar to pLCAT in the extent and structure of its glycosylation.

As LCAT glycosylation structure varied with its source, the influence of LCAT source on enzyme function was evaluated. LCAT kinetics demonstrated small differences in apparent K_m. bLCAT consistently had a 3-fold smaller apparent K_m than that of pLCAT, whereas the apparent K_m of CHO LCAT was intermediate. The maximum specific activity of bLCAT was 3-fold lower than that of pLCAT, whereas the apparent V_{max} for CHO LCAT was the same as that of pLCAT. Collet and Fielding (5) observed that LCAT expressed in the presence of glucosidase inhibitors had a decreased apparent V_{max} (0.15 ± 0.06 vs. 0.64 ± 0.14 nmol/h per ml for glucosidase inhibited and native enzyme, respectively) and no change in apparent K_m (19.3 ± 3.3 vs. 21.4 ± 3.0 mM, respectively), suggesting that type of glycosylation could affect catalytic rate. In mutagenesis studies, reduction in apparent V_{max} but not apparent K_m was observed when N84 was mutated (4, 7, 25). When N384 was mutated, the apparent V_{max} remained the same (N384T) or increased (N384Q) (4, 7, 25). However, the apparent K_m for the N384T mutant decreased, whereas no change or a slight increase was observed for the N384Q mutant. Taken together, these studies suggest that extent of glycosylation affects LCAT catalytic rate and support our results that apparent V_{max} is affected by the extent and type of glycosylation.

The source of LCAT also may have a minor influence on substrate fatty acyl specificity. Human plasma LCAT has a 1.6-fold greater activity against rHDL-containing POPC compared to PAPC. This is similar to the difference in apparent V_{max} for human plasma LCAT observed by Jonas et al. (26) for rHDL-containing POPC versus PAPC (101 vs. 79 nmol cholesteryl ester formed/h, respectively). Even though bLCAT and HepG2 LCAT specific activities against POPC- and PAPC-containing substrates were reduced, the order of substrate fatty acyl specificity was maintained in all of the enzymes examined. Qu et al. (7) compared the apparent V_{max} and apparent K_m values of their glycosylation mutants against POPC and DAPC substrates. Although catalytic rates decreased with N84T and apparent K_m decreased with N384T, the enzymes maintained their preference for POPC over PAPC, suggesting that N-linked glycosylation of LCAT had no major influence on substrate fatty acyl specificity. Francone, Evangelista, and Fielding (8) demonstrated that mutating N272 significantly altered the ratio of phospholipase to transacylase activity, causing LCAT to become a phospholipase with little acyltransferase activity. No such changes were observed with the baculoviral-expressed LCAT or the CHO-expressed LCAT. Both bLCAT and CHO LCAT have the same phospholipase to acyltransferase ratio as plasma LCAT, suggesting that altering the glycosylation of bLCAT did not alter the enzyme mechanism.

These data suggest that the interaction of bLCAT and HepG2 LCAT with substrate, either at the rHDL interface or the molecular substrate level, is different from that of plasma-derived LCAT. The structure, composition, and amount of glycosylation most likely have an indirect effect on the overall structure of LCAT, thus influencing the active site, the interfacial binding site and/or the activation of LCAT.

This work was supported by grants from the National Heart, Lung, and Blood Institute (HL49373), an American Heart Association Grant in Aid (91008310), and by a fellowship (K.R.M.) from the North Carolina affiliate of the American Heart Association (NC-94-FW-07). The authors gratefully acknowledge the technical assistance of Abraham Gebre and the editorial assistance of Karen Klein. Goat anti-LCAT polyclonal antibody was generously provided by Dr. Henry Pownall of the Baylor College of Medicine, Houston, Texas. Anti-LCAT monoclonal antibody was generously provided by Dr. Yves Marcel, University of Ottawa Heart Institute, Ottawa, Ontario, Canada.

Manuscript received 30 August 1995 and in revised form 4 December 1995.

Downloaded from www.jlr.org by guest, on June 18, 2012

REFERENCES

1. Norum, K. R., E. Gjone, and J. A. Glomset. 1989. Familial lecithin:cholesterol acyltransferase deficiency, including fish eye disease. *In* The Metabolic Basis of Inherited Disease. C. R. Scriver, A. L. Beaudet, W. S. Sty and D. Valle, editors. McGraw-Hill Information Services Co., New York, NY. 1181–1191.
2. Doi, Y., and T. Nishida. 1983. Microheterogeneity and physical properties of human lecithin-cholesterol acyltransferase. *J. Biol. Chem.* **258:** 5840–5846.
3. Fielding, C. J. 1990. Lecithin:cholesterol acyltransferase. *In* Advances in Cholesterol Research. M. Estahani and J. Swaney, editors. Telford Press, Caldwell, NJ. 270–314.
4. Karmin, O., J. S. Hill, X. Wang, R. McLeod, and P. H. Pritchard. 1993. Lecithin:cholesterol acyltransferase: role of N-linked glycosylation in enzyme function. *Biochem. J.* **294:** 879–884.
5. Collet, X., and C. J. Fielding. 1991. Effects of inhibitors of N-linked oligosaccharide processing on the secretion, stability and activity of lecithin:cholesterol acyltransferase. *Biochemistry.* **30:** 3228–3234.
6. Schindler, P. A., C. A. Settineri, X. Collet, C. J. Fielding, and A. L. Burlingame. 1995. Site-specific detection and structural characterization of the glycosylation of human plasma proteins lecithin:cholesterol acyltransferase and apolipoprotein D using HPLC/electrospray mass spectrometry and sequential glycosidase digestion. *Protein Sci.* **4:** 791–803.
7. Qu, S. J., H. Z. Fan, F. Blanco-Vaca, and H. J. Pownall. 1993. Effects of site directed mutagenesis on the N-glycosylation sites of human lecithin:cholesterol acyltransferase. *Biochemistry.* **32:** 8732–8736.
8. Francone, O. L., L. Evangelista, and C. J. Fielding. 1993. Lecithin-cholesterol acyltransferase: effects of mutagenesis at N-linked oligosaccharide attachment sites on acyl acceptor specificity. *Biochim. Biophys. Acta.* **1166:** 301–304.
9. Villareal, X. C., K. G. Mann, and G. L. Long. 1989. Structure of human osteonectin based upon analysis of cDNA and genome sequences. *Biochemistry.* **28:** 6483–6491.
10. Kelm, R. J., and K. G. Mann. 1991. The collagen binding specificity of bone and platelet osteonectin is related to differences in glycosylation. *J. Biol. Chem.* **266:** 9632–9639.
11. Opdenakker, G., P. M. Rudd, C. P. Ponting, and R. A. Dwek. 1993. Concepts and principles of glycobiology. *FASEB J.* **7:** 1330–1337.
12. Kornfeld, R., and S. Kornfeld. 1985. Assembly of asparagine-linked oligosaccharides. *Annu. Rev. Biochem.* **54:** 631–664.
13. Tabor, S., and C. C. Richardson. 1987. DNA sequence analysis with a modified bacteriophage T7 DNA polymerase. *Proc. Natl. Acad. Sci. USA.* **84:** 4767–4771.
14. Sorci-Thomas, M., M. W. Kearns, and J. P. Lee. 1993. Apolipoprotein A-I domains involved in lecithin-cholesterol acyltransferase activation. *J. Biol. Chem.* **268:** 21403–21409.
15. Chen, C. H., and J. J. Albers. 1985. A rapid large-scale procedure for purification of lecithin:cholesterol acyltransferase from human and animal plasma. *Biochim. Biophys. Acta.* **834:** 188–195.
16. Matz, C. E., and A. Jonas. 1982. Reaction of human lecithin:cholesterol acyltransferase with synthetic micellar complexes of apolipoprotein A-I, phosphatidylcholine and cholesterol. *J. Biol. Chem.* **257:** 4541–4546.
17. Parks, J. S., T. Y. Thuren, and J. D. Schmitt. 1992. Inhibition of lecithin:cholesterol acyltransferase activity by synthetic phosphatidylcholine species containing eicosapentaenoic acid or docosahexaenoic acid in the *sn*-2 position. *J. Lipid Res.* **33:** 879–887.
18. Bligh, E. G., and W. J. Dyer. 1959. A rapid method of total lipid extraction and purification. *Can. J. Biochem. Physiol.* **37:** 911–917.
19. Laemmli, U. K. 1970. Cleavage of structural proteins during the assembly of the head of bacteriophage T4. *Nature.* **227:** 680–685.
20. Oakley, B. R., D. R. Kirsch, and N. R. Morris. 1980. A simplified ultrasensitive silver stain for detecting proteins in polyacrylamide gels. *Anal. Biochem.* **105:** 361–363.
21. Chawla, D., and J. S. Owen. 1995. Secretion of active human lecithin:cholesterol acyltransferase by insect cells infected with a recombinant baculovirus. *Biochem. J.* **309:** 249–253.
22. Crowl, R. M., T. J. Stoller, R. R. Conroy, and C. R. Stoner. 1991. Induction of phospholipase A_2 gene expression in human hepatoma cells by mediators of the acute phase response. *J. Biol. Chem.* **266:** 2647–2651.
23. Fraser, M. J. 1992. The baculovirus-infected insect cell as a eukaryotic gene expression system. *Curr. Top. Microbiol. Immunol.* **158:** 131–172.
24. Tarentino, A. L., and T. H. Plummere, Jr. 1994. Enzymatic deglycosylation of asparagine-linked glycans: purification, properties and specificity of oligosaccharide-cleaving enzymes from *Flavobacterium meningosepticum. Methods Enzymol.* **230:** 44–57.
25. Karmin, O., T. S. Hill, and P. H. Pritchard. 1995. Role of N-linked glycosylation of lecithin:cholesterol acyltransferase in lipoprotein substrate specificity. *Biochim. Biophys. Acta.* **1254:** 193–197.
26. Jonas, A., N. L. Zorich, K. E. Kezdy, and W. E. Trick. 1987. Reaction of discoidal complexes of apolipoprotein A-I and various phosphatidylcholines with lecithin:cholesterol acyltransferase. Interfacial effect. *J. Biol. Chem.* **262:** 3969–3974.

Downloaded from www.jlr.org by guest, on June 18, 2012